

The chemistry behind the first Portuguese postage stamps (1853–1894). A non-destructive analytical and chemometric analysis of pigments, fillers and binders

Simone C.R. Ferreira, Martina Franchi, Alberto A.C.C. Pais, J. Sérgio Seixas de Melo^{*}

University of Coimbra, CQC - IMS, Department of Chemistry, 3004-535, Coimbra, Portugal

ARTICLE INFO

Keywords:

Postage stamps. pigments. dyes. XRF. ATR-FTIR. UV-Vis. Chemometrics

ABSTRACT

The analysis of 28 specimens of some of the first Portuguese postage stamps, dated from 1853 to 1894, was undertaken with non-destructive techniques: X-Ray fluorescence (XRF), Attenuated Total Reflection Fourier Transform Infrared (ATR-FTIR) and Ultraviolet–Visible Reflectance Spectroscopy (UV–Vis). Ink, paper and cancellation of the postage stamps were analysed, and the pigments, binders and fillers identified. Prussian blue was found present in all blue and also in green and brown specimens. Chrome and zinc yellow, lead sulphate and mars red were also found in other of the investigated postage stamps. Binders consist mostly of protein glue. Fillers such as calcite and kaolinite were found dominant. The presence of the latter served as an indicator for distinguishing between genuine and forged samples. UV–Vis spectra also proved useful for the same purpose. All the above information was processed and organized using chemometric techniques. These include mainly Hierarchical Cluster Analysis (HCA), for clustering stamps of similar composition, and Principal Component Analysis (PCA) for mapping the samples and identifying the more relevant variables. The latter are, in the paper, content of calcium, potassium, sulphur and silicon and, in the dye pigment area, of iron, zinc and lead content. The study introduces an approach in which, by combination of non-destructive multi analytical techniques with chemometric analysis, extensive information on different aspects of the composition of the studied postage stamps is provided, including that of paper and dyes.

1. Introduction

Identification of the constituents used in the making of works of Art, namely paintings, painted sculptures or illuminated manuscripts (e.g. in medieval books) is indispensable for understanding art evolution. It also facilitates rigorous restoration of works and identification of potential forgeries. Included in this group of works of Art are postage stamps, in particular those printed in first production years.

Postage stamps are printed paper documents that have been issued by governments since 1840 as prepayment for a mail delivery service to be rendered by an official governmental agency [1]. They are considered part of the Cultural Heritage of a country, due to its historical and social value and constitute a type of art work, which is, in some cases, very rare and precious.

After the successful postal reform in Great Britain, in 1840, which introduced the adhesive postage stamp, Queen Victoria's famous Penny Black (1843) was the first to be produced. The idea came from Sir

Rowland Hill, a member of the UK Parliament, who proposed the postage stamps in order to make the sender pay for the mail fare, to face the problem of a huge number of returns from the recipients, who was supposed to pay for it [2]. The Swiss Cantons Zurich and Geneva followed and issued stamps in 1843 [3]. Some postmasters in the USA issued stamps starting in 1845. The first official issue was the next, in 1847 [4]. Also, in the same year, the famous first stamps of Mauritius were printed [5]. This has a domino effect throughout Europe with the first German stamp, the black Bavarian Kreuzer, to be issued in 1849 in Bavaria [6], and the first French postage stamps created a few months after the proclamation of the Second Republic and issued in 1849; these stamps were engraved with the head of the goddess of agriculture, Ceres, symbol of liberty and the Republic, and later with the head of Louis Napoleon Bonaparte, president of the French Republic [7].

Portugal had its Postal services restructured in 1851 and, in 1852, the English system was adopted. The first postage stamps were produced in Portugal in 1853, with the effigy of the Portuguese queen, Mary the

^{*} Corresponding author.

E-mail address: sseixas@ci.uc.pt (J.S. Seixas de Melo).

2nd (Maria II) [8].

Stamps have not been scientifically studied to the same extent as other cultural items such as lithographs, coins, etc. The history of materials employed in the manufacture of stamps is still lacking information, because only a minor fraction of the world production has been investigated.

Analysis of Portuguese postage stamps has been carried out in only a few studies. The respective dye/pigment composition was investigated, focused in the molecules of colour used in some of the postage stamps of the period 1857–1909 [9]. Similar strategies were employed to investigate the presence of the mauveine dye in a set of historical samples and in lilac postage stamps from the Victorian period [10].

A postage stamp comprises several layers, including adhesive, paper, coating on the printed side, and the printing ink itself. A cancelled stamp may also have all or a portion of the cancellation [11]. Thus, an in-depth study of postage stamps must consider paper, ink and gum chemistry, as well as colour (the colouring agent) and chemical aspects of printing.

Non-destructive XRF analysis is one of the most widely used and versatile of all the existent instrumental analytical techniques. For postage stamps, however, it should be expected that the XRF spectrum will include elements from all the layers of the stamp: ink, cancellation, paper, gum, and any residual backing material [12].

Different authors have worked on the identification of the chemical composition of stamps using this technique, in combination with others such as ATR-FTIR [12,13].

Another approach, combining non-destructive micro-Raman and micro-XRF analysis, has been proposed for the examination of Spanish postage stamps with denomination of 15 cents containing colour errors and belonging to the King Alfonso III issue (from 1889 until 1901). The goal of the work was to verify the authenticity of the investigated specimens and to propose an explanation for the generation of the colour errors [14].

Raman and ATR-FTIR, vibrational techniques, have provided the results in the analysis of inks in an extensive study, covering more than 150 years, of stamps of the Italian Kingdom and Republic [15]. This followed a previous work in which ATR-FTIR was employed in the analysis of paper and glue components. In this work, one of the most famous Italian stamps, the so-called “Gronchi Rosa” (Pink Gronchi), and a certified fake sample were also investigated. The results showed one fundamental difference between the two samples: the absence of kaolin signals in the forged postage stamp [16].

Raman spectroscopy was employed again on Chinese postage stamps specimens, to investigate, non-destructively, six Imperial China Engraved Coiling Dragon stamps. Results showed that some pigments were intentionally mixed to produce a whole different hue or colour [17].

For the study of pigments in the printing inks employed in the first hand engraved Japanese postage stamps, XRF combined with FTIR and Raman were the spectroscopic techniques used. This work has revealed, for the first time, the changes of the pigments used for all colours of the stamps issued during 1871–1876, and it has been recognized that a drastic change in the ink composition occurred in 1872, when the printing of the postage stamps was transferred from a private printer, Matsuda, to the Government [18].

Through the use of ATR-FTIR the composition of inks used to print the many different types of United States one-cent Benjamin Franklin stamps of the 19th century has been established. This information allowed a historical evaluation of the formulations used in different time periods, and also facilitates the making of a clear differentiation amongst the various postage stamps [19].

The combination of XRF and Raman spectroscopy was also used to address hyperinflation German stamps in what concerns the identification of dyes and pigments [20]. Similar techniques were used to characterize the pigments and paper in Ottoman specimens [21].

The results obtained from the study of different materials used in the production of Argentine postage stamps, from 1888 to 2016, explains

how the use of these materials changed over time. Analyses of more than 40 Argentine postage stamps were carried out in situ using portable X-ray fluorescence spectroscopy (p-XRF) and ATR-FTIR. Paper, ink, coatings, and adhesives were analysed and the period of use of each material was established [13].

Studies with emphasis on Forensics have also captured the interest of researchers. These include diverse efforts on authentication [22,23] and identification of forged specimens [24]. A thorough study on the precious Hawaiian Missionary items has been carried out using Raman microscopy [25]. A comparison was made, with forged specimens, focusing on the use of inks and of a pigment intended to imitate aging effects on the paper. The same authors extended later their investigations to postage stamps from Mauritius [5]. Both contributions propose a sort of palette for original specimens against which suspicious items have to be contrasted.

Chemometrics provides excellent statistical tools for a better understanding of the chemical data facilitating the identification of the main patterns in terms of specimen similarity and composition, providing a clear picture of the whole set of stamps.

In the present work, the study of some of the first Portuguese postage stamps is made, with the main purpose of elucidating their chemical composition using a non-destructive analysis. This is made with the identification of their dyes/pigments, together with additives (fillers and binders) and paper characteristics from spectral data from XRF, ATR-FTIR, UV-Vis followed by data scrutiny with PCA and HCA. The analyses made allowed to identify, as major colorant materials, the pigments Prussian blue and lead sulphate, and the identification of forged specimens.

2. Experimental section

2.1. Materials and methods

2.1.1. Samples

In this work, the postage stamps under analysis consist of 23 Portuguese specimens and 5 from its former colonies, one from Cape Verde, 4 (1 real and corresponding forgery, and 2 additional forgeries) from São Tome and Príncipe. The time period of the sampling spans the years 1853–1894.

The objective is to study a relatively inhomogeneous set of postage stamps with different colours so as to contrast the respective compositions. At the same time, one colour is dominant, potentially allowing to identify variations in composition within the same colour. The description of the samples can be found in Table 1. The production or printing date is made according to the Yvert and Tellier catalogue [26]. Fig. 1 gathers images of some of the most representative postage stamps. The rest of the samples, studied in this work, are presented in Fig. S1 of SI.

Each sample, subject to analysis, consisted of 1–3 postage stamps. When more than one postage stamp was available, data was acquired for the different specimens; when only one exemplar was available, 2–3 acquisitions were made for each postage stamp. Duplicates and triplicates were used for reproducibility assessment in XRF semi-quantitative measurements. It was additionally checked by assessing proximity of the replicates in the Euclidean distance dendrogram which is presented in Fig. S3. For the remaining techniques, replicas were used to check of the presence of the same vibrational wavenumber values and the same overall absorption spectral behaviour.

The samples were analysed in three positions: one representative of the region containing the dye/pigment and paper, other representing locations with the appearance of neat paper and finally another representing the cancellation (upon paper or upon the printed area), when existent.

Table 1

Sample description of the 28 investigated samples. The color is based in a visual analysis and the label (from #1 to #28) facilitates the identification process in the present work.

Catalogue number	Color	Effigy ^(a)	Rate	Print date	Origin	Label
1	Black	Crown seal	5r	1870–77	São Tome and Principe	#1
1	Black	Crown seal (fk)	5r	1870–77	São Tome and Principe	#2
2	Blue	D. Maria II	25r	1853	Portugal	#3
3	Green	D. Maria II	50r	1853	Portugal	#4
3	Brown	Crown seal (fb)	20r	1870–77	São Tome and Principe	#5
3	Yellow	Crown seal (fy)	20r	1870–77	São Tome and Principe	#6
6	Blue	D. Pedro V	25r	1855–56	Portugal	#7
6	Blue	D. Pedro V	25r	1855–56	Portugal	#8
7	Green	D. Pedro V	50r	1855	Portugal	#9
8	Lilac	D. Pedro V	100r	1855	Portugal	#10
9	Brown yellowish	D. Pedro V	5r	1856	Portugal	#11
12	Rose	D. Pedro V	25r	1856	Portugal	#12
13	Brown	D. Luís I (profile)	5r	1862	Portugal	#13
14	Orange	D. Luís I (profile)	10r	1862	Portugal	#14
14	Blue	Crown	50r	1881–85	Cape Verde	#15
15	Rose	D. Luís I (front)	25r	1862–66	Portugal	#16
16	Green	D. Luís I (profile)	50r	1862	Portugal	#17
24	Lilac	D. Luís I (profile)	100r	1868	Portugal	#18
25	Blue	D. Luís I (profile)	120r	1866–67	Portugal	#19
25	Blue	D. Luís I (profile) (fn)	120r	1866–67	Portugal	#20
25	Blue	D. Luís I (profile) (fo)	120r	1866–67	Portugal	#21
50	Olive green	Jornaes (rs)	2 ^{1/2} r	1876–94	Portugal	#22
50A	Yellowish olive green	Jornaes (bs)	2 ^{1/2} r	1876–94	Portugal	#23
54	Greyish blue	D. Luís I (profile)	25r	1880–81	Portugal	#24
59	Brown	D. Luís I (profile)	25r	1882–87	Portugal	#25
60	Lilac rose	D. Luís I (front)	25r	1882–87	Portugal	#26
70	Green	D. Carlos I	25r	1892–93	Portugal	#27
71	Ultramarine	D. Carlos I	50r	1892–93	Portugal	#28

^a Fake samples include, additionally, fk (general fake), fb (brown color, fake), fy (yellow color, fake), fn (more recent fake), fo (older fake), rs (red cancellation), bs (black cancellation).

2.2. Analytical techniques

2.2.1. XRF spectrometry

For elemental, qualitative and semiquantitative analysis, a high-sensitivity energy dispersive Hitachi device, model SEA6000VX, was used. The equipment possesses an X-ray tungsten target tube and a silicon multi-cathode detector.

In qualitative analysis, spectra were recorded with two different tube voltages, 15 kV and 50 kV, with a tube current of 1000 μ A, in air environment and with an acquisition time of 60 s. Each measurement was made in a sampling area of 0.5×0.5 mm². Spectra were acquired and processed using the X-ray station software in counts per second (cps). The semiquantitative analyses were made with the same programme in the bulk analysis (full parameters) application mode. The number of set conditions were different depending on the elements to be measured. Typically, three to four different sets were applied in the analysis. The measuring time, the environment and the sampling area were kept constant. Another software, denoted mapping station, was used to obtain mapping results. In this, certain conditions as the scan size, the voltage and current of the tube, the use of filter, the pixel size, the collimator and, finally, the time per pixel must be established. The results are typically obtained in ppm.

2.2.2. ATR-FTIR

The Thermo Scientific™ Nicolet™ iN™10 Infrared Microscope in ATR mode was used in molecular analysis. The ATR crystal was made of germanium and the mercury cadmium telluride (MCT) detector was cooled with liquid nitrogen.

Because of the non-destructive nature of the setup, every single stamp was directly placed onto the ATR window with no further preparation. For each sample, 256 scans were recorded in the 4000–650 cm^{−1} spectral range with a 2 cm^{−1} resolution. Spectral data were acquired using the OMNIC v8.0 (Thermo Electron Corp.) software without

post processing.

The ATR-FTIR results were analysed using a spectral collection of over 150 ATR-FTIR spectra of materials related to Cultural Heritage and conservation science [27]. They were measured in the 4000–80 cm^{−1} mid-IR and far-IR regions.

2.2.3. UV–Vis

The UV–Vis absorption spectra of the samples were acquired using a spectrophotometer from Agilent technologies, model Cary 5000 UV–Vis–NIR. The measurements were made using a module specific for solids, with a sample holder that preserves the integrity of the specimens.

The absorption spectra (in wavelength units) was recorded at room temperature (T = 293 K). Note that the obtained data are obtained in the reflection mode of the equipment and further converted into absorption using the equipment's software based in the Kubelka-Munk correction. All data were collected between 200 and 800 nm with spectral resolution of 1 nm. The acquisition was made using Cary Win UV v6.0 software.

UV–Vis results were also compared with a Fibber Optics Reflectance Spectra (FORS) database of 54 historical pigments commonly used in art works [28].

2.3. Chemometric and graphical tools

Data treatment was made using the R programming language (version 4.0.2) upon the IDE RStudio (version 1.3.959). Two main chemometric techniques were used in this work, Hierarchical Cluster Analysis and Principal Component Analysis.

The hierarchical clustering method groups data objects into a tree of clusters. In this work, an agglomerative method was used. It starts an iterative process from the initial situation where each data point is considered as a separate cluster and form the hierarchical composition



Fig. 1. Three examples of the most representative and oldest Portuguese postage stamps. (Left) Stamp #3; (center) stamp #4 and (right) stamp #7. For labelling, please see Table 1.

in a bottom up fashion by merging the clusters. Merging is done on the basis of the mutual distances between the clusters. A number of linkage-rules can be applied to express the distance between clusters. In this work, Ward's method was selected because it generally originates well defined clusters. This analysis is graphically represented in the form of a dendrogram [29]. For every identified clusters, the average composition was calculated and represented in a circular barplot.

The most important use of the PCA method is to represent the n -dimensional data structure in a smaller number of dimensions, preferentially two or three. This allows to observe groupings of objects and outliers which define the structure of the data set. In the PCA model, new variables are now found, giving a clear picture of the variability of the data. A graphical picture of the PCA results is the biplot, where the objects are represented in the new coordinates, together with the main direction of the original variables [30]. In the mathematical procedure, underlying the method, no scaling was introduced in the variance matrix.

HCA and PCA were applied exclusively to XRF results.

Finally, an heatmap was used to represent wavenumber matching in section 3.2.

3. Results and discussion

3.1. XRF

The semi-quantitative analysis of the XRF data (see experimental section for details) was obtained for all the postage stamps analysed. This provides measurements expressed in the form of a concentration with an estimate of the respective uncertainty for each element. Only those showing less than 40% uncertainty were considered. See Fig. 2 for an illustrative example of a XRF spectrum. The bands corresponding to each identified element are indicated.

All samples were, subsequently to the XRF analysis, subjected to mapping. For each sample, the elements identified in the semi-quantitative analysis were inspected, which also allowed to set the mapping voltage, 15 kV or 50 kV. Typically, more than 5 elements were scanned in each sample. XRF mapping results in a 2-D image and comprises the whole surface of the postage stamp. The mapping provides information on the distribution of the element under analysis on the postage stamp. Two general situations appear: one, in which the element is present in the printed area and, another, in which the element is more or less uniformly scattered upon the surface. The former suggests that the element is found in the dye/pigment of the ink, whereas the latter indicates that the element is present in the paper matrix or can be a coating pigment. A third, less common situation arises, in the samples under observation, when the pattern of the postmark is visible in the mapping image. Data in Fig. 3 represents selected examples of these three situations.

Fig. 3 A presents the image for sample #19, a blue postage stamp

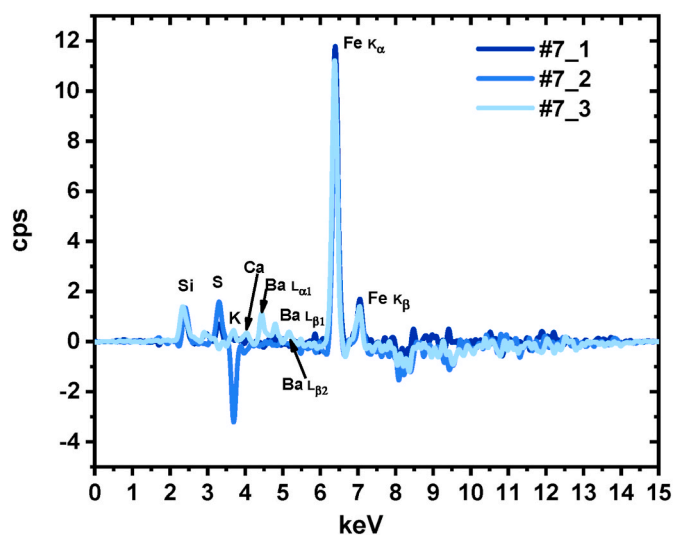


Fig. 2. XRF spectra obtained at 15 kV for postage stamp #7. For labelling, please see Table 1.

printed in the period 1866-67. Panels (a) and (b) depict some of the data corresponding to the XRF mapping. These indicate the presence of iron and lead in the blue printed area, especially visible in the case of iron, in which the lettering is readable (Fig. 3 (a)). These observations suggest that the two elements are associated with the pigment, thus indicating the presence of Prussian blue ($\text{Fe}_4[\text{Fe}(\text{CN})_6]_3$), and lead sulphate (PbSO_4). Note that sulphur is also present in the mapping results (data not shown). Lead and sulphur can be part of the constituents of various lead sulphate compounds, palmierite ($\text{K}_2\text{Pb}(\text{SO}_4)_2$), anglesite (PbSO_4), lanarkite ($\text{Pb}_2(\text{SO}_4)\text{O}$), leadhillite ($\text{Pb}_4\text{SO}_4(\text{CO}_3)_2(\text{OH})_2$), that are white pigments, and galena (PbS), that is a black pigment. Since the stamp is blue and, in the literature, there is no evidence for the use of galena for the printing postage stamps, the suggestion of lead sulphate seems to be the most adequate one [31]. In what concerns the presence of Prussian Blue, this is further corroborated by the signal corresponding to the $\text{C}\equiv\text{N}$ stretching mode at 2087 cm^{-1} [32] (Fig. 4).

Panels (B), (c) and (d) show the corresponding image and mapping, now for sulphur and barium, obtained for sample #27. This is a striking example of elements that are detected in high amounts, in the form of a filler or a coating pigment. Indeed, they are found uniformly distributed upon the surface of the postage stamp. Interestingly, even the perforations are clearly visible.

Another interesting example is provided by sample #22, in panels (C), (e) and (f) of Fig. 3. In this case, sulphur, chlorine, chromium and iron are found in the printed area, i.e., in the pigment region. In turn, lead is found both in the printed area and in the specific region of the red

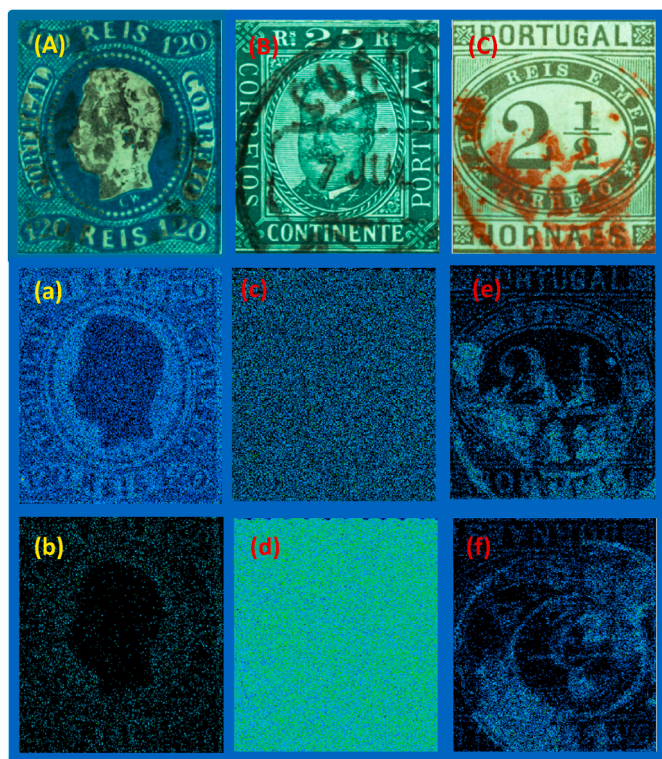


Fig. 3. Stamp image and XRF mapping images for (A) #19, (a) Fe scanning at 15 kV and (b) Pb, 50 kV; (B) #27, (c) S scanning at 15 kV, and (d) Ba, 50 kV and (C) #22, (e) S scanning at 15 kV, and (f) Pb, 50 kV. For labelling, please see Table 1.

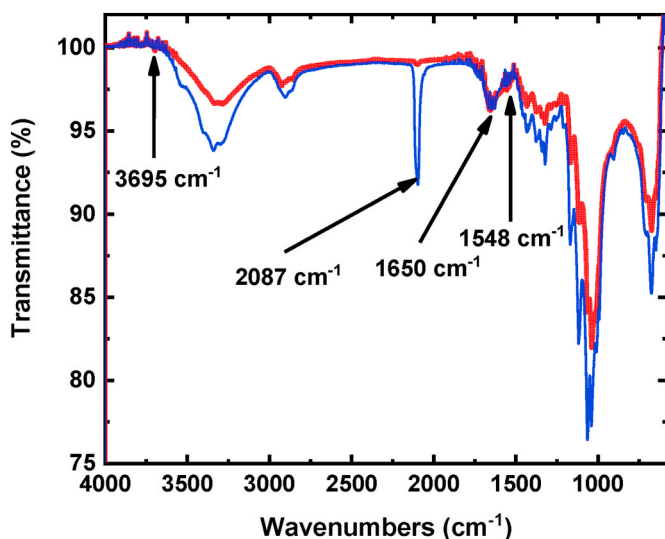


Fig. 4. ATR-FTIR spectra obtained for sample #19. Lines are blue for the dye and paper matrix and red for the paper alone. For labelling, please see Table 1. The most representative vibrational modes are indicated. For more details please see text.

cancellation, meaning that it is part of the composition of both the pigment and cancellation. The sample displays an olive-green color. With the elemental composition determined, we have to conclude that the color results, at least, from a mixture of blue and yellow pigments. The mapping indication that these elements are present in the printed area shows that they must be part of the composition of the pigments involved. As the blue color is due to Prussian blue, the only yellow

pigment that contains lead and chromium is chrome yellow (PbCrO_4). The olive hue was obtained with one additional pigment, lead sulphate, as inferred from the presence of lead and sulphur. The cancellation present in sample #22 (Fig. 3 C) is likely to be based in the red lead (Pb_3O_4) pigment.

Contrasting with this #22 postage stamp, the XRF data, in general, does not provide good evidence for the composition of cancellations. When inspected upon paper, the signals were found similar to that of paper, and the same situation occurs if inspected upon the printed area. This is probably a consequence of the cancellation appearing in a very thin layer. As such, analysis of the corresponding cancellation matrix could not be further pursued in this work.

3.2. ATR-FTIR

The postage stamps were subjected to ATR-FTIR analysis; see Fig. 4 for an illustrative example of an ATR-FTIR spectrum. In this, the signalled wavenumbers are responsible for the identification of kaolinite (3695 cm^{-1} , O–H stretching frequency associated with hydroxyl ions) [16], Prussian blue (2087 cm^{-1} , $\text{C} \equiv \text{N}$ stretching) [32] and protein glue (1650 cm^{-1} , amide I band associated with the C–N stretching and N–H bending vibrations of the peptide groups, and 1548 cm^{-1} , amide II band associated with the stretching of N–H and vibration of C–N) [33,34].

The ATR-FTIR spectra for all the other studied postage stamps is given in Fig. S2.

3.3. UV–Vis

Absorption spectra were also obtained for the 28 investigated samples, both in dye/pigment and paper areas. The latter was used as reference to check if the dye/pigment is detected. An example is presented in Fig. 5. For interpreting the spectra, a comparison was made with those from a spectral database from ref. [28]

In eight of the samples, it was not possible to distinguish between the spectrum of the dye/pigment and that of the paper. Samples with visual black (#1, #2), blue (#3), brown (#5, #25), green (#27), olive green (#22) and yellow (#6) colours formed this group. A possible explanation for these findings, is likely to be due to the little amount of dye/pigment present. In those (#4, #7, #8, #9, #10, #11, #12, #13, #14, #15, #16, #17, #18, #19, #20, #21, #23, #24, #26, #28) where the spectra are not completely deprived of features, these are generally of low intensity. For specimens with the same colour, the spectra exhibit large variations, even if a common pigment is present. They also produce

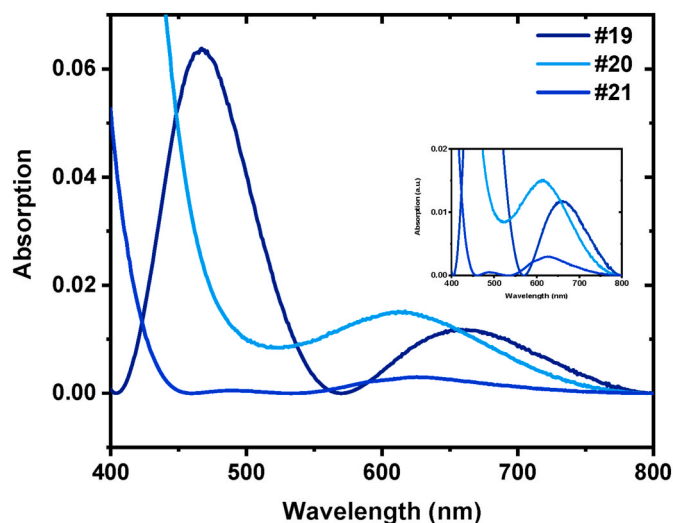


Fig. 5. UV–Vis spectra of sample #19 and respective fakes. The insert presents an amplification in the absorption axis.

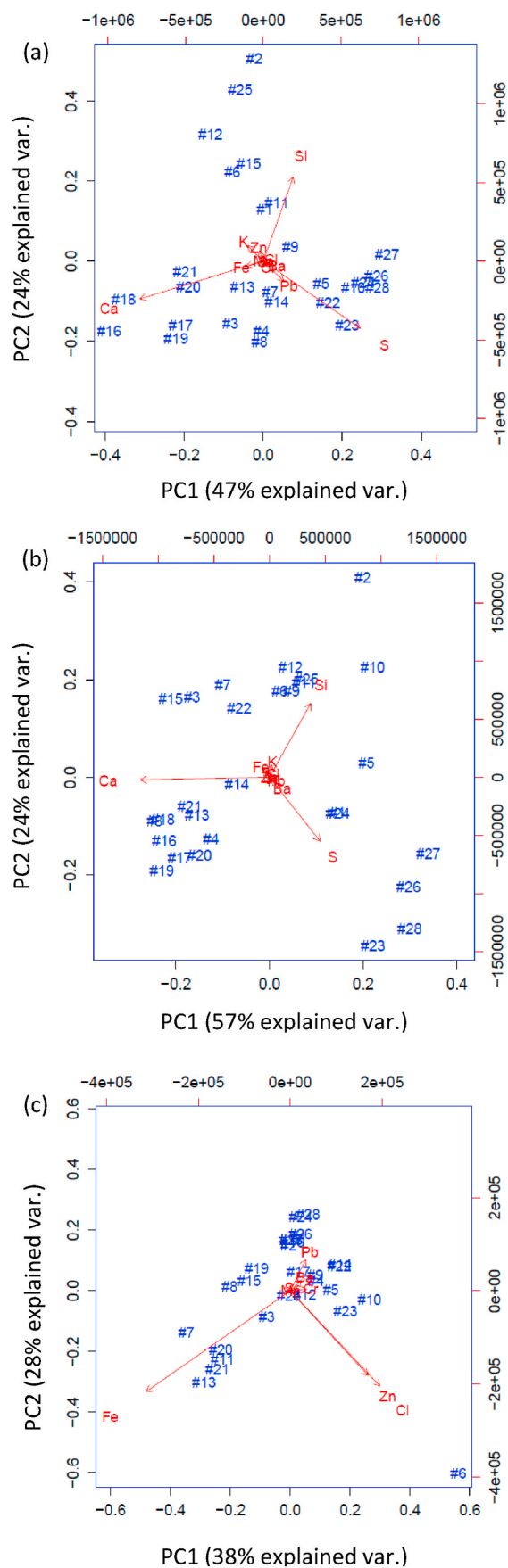


Fig. 6. Biplot using covariance matrix for (a) dye_paper, (b) paper and (c) dye_paper, excluding information from Ca, K, S and Si. For labelling, please see Table 1.

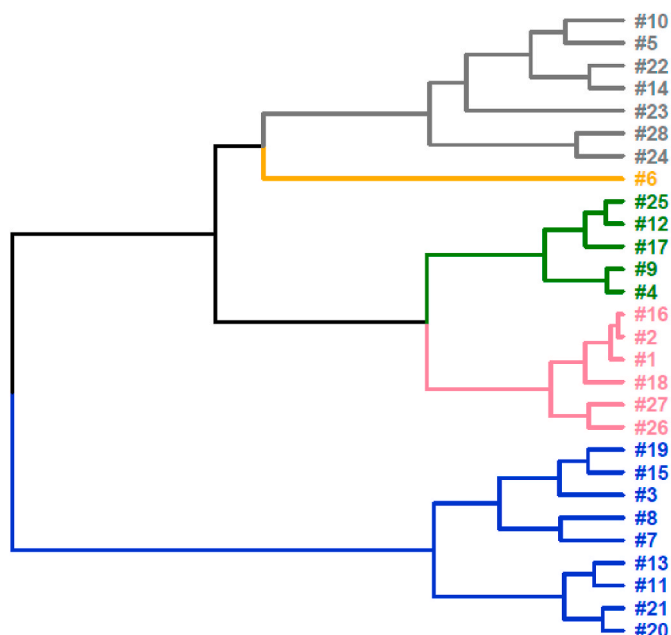


Fig. 7. Dendrogram obtained with Ward's linkage the average value for each sample. The clusters (in different colours) are numbered from 1 to 5. For labelling, please see [Table 1](#).

spectra clearly different from that of the pigment itself applied in watercolour paper [28], which may result from the presence of other stamps' constituents. This is seen, for example, with Prussian blue. Five samples (#7, #8, #15, #20, #28) are characterized by a single broad band, located from values close to 570 nm to values exceeding 610 nm. When two bands are present, one is found with wavelength values ranging from 467 to 532 nm (this for a greyish blue sample, #24) and another band between 626 and 670 nm.

In which concerns the postage stamps with green and brown visual colour, it is apparent that they result from a mixture of different pigments, chrome yellow and Prussian blue, as previously seen from the

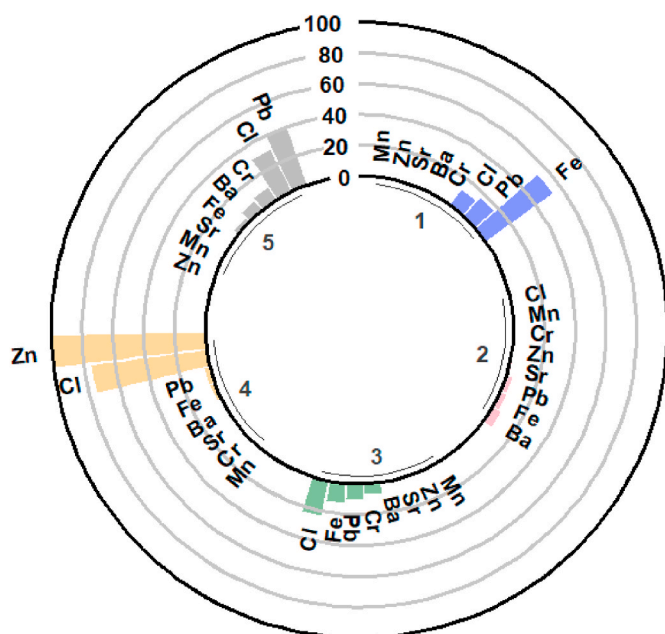


Fig. 8. Circular bar plot with the composition of the five clusters. Data is presented as percentage of the most prevalent element (Zn), considering all clusters in Fig. 7. The plot was obtained with the ggplot function in R.

XRF and ATR-FTIR analysis. All visually green postage stamps display a band with maxima at ca. 630 nm. Only in one case (#4), two bands are visible with wavelength maxima at 586 and 632 nm. Once again, there is no similarity between the spectra of the postage stamps and those of the pigments.

The two brown samples (#11, #13) are consistent in composition, with the presence of Prussian blue, chrome yellow and red lead or mars red, with the spectra display in a single band varying from 522 to 532 nm, with no direct correspondence with the spectra of the pigments.

In one of the lilac samples (#10), three bands are visible, at 520, 560 and 660 nm. In the other only the central band is visible (560 nm).

The two rose stamps (#12, #16) exhibit very similar spectra, with bands in the vicinity of 486, 522 and 562 nm, suggesting that common components are present. The fact that no element stands out in XRF mapping, together with the low content reported for the elemental composition suggests that the colouring matter is probably an organic dye.

Overall it may be considered that this technique provides, in some cases, less informative data. This should, however, be regarded with caution. Indeed, and taking as example postage stamp #19, for which a genuine and two forged specimens (#21 and #22) are available, it can be seen that UV-Vis spectra clearly distinguish the genuine from the forged item (Fig. 5).

3.4. Chemometric analysis

Subsequent analysis based on HCA and PCA is performed aiming to establish the structure of the XRF data. A first attempt to use HCA to rationalize these results was made using data collected from the three different locations, corresponding to three matrices, in the postage stamps: (i) dye_paper, (ii) paper, and (iii) cancellation. The first matrix leads to a dendrogram with no visible structure, thus showing that the different colours of the samples are not duly organized. The corresponding biplot based on the XRF analysis, Fig. 6 (a), shows that the elements silicon, sulphur and calcium are responsible for the data structure. Analysis of the (ii) paper matrix reveals the same overall behavior, with silicon, sulphur and calcium as the major players, as seen in Fig. 6 (b). This indicates that these elements are essentially present in the paper matrix. Also, a direct inspection of the data indicates that potassium is present, in almost equal amounts, in both matrices, again suggesting that it is a relevant component of the paper.

A new dendrogram was therefore produced by removing the data corresponding to these elements from the `dye_paper` results matrix. The new data now more closely characterizes the information relative to pigment elements. Fig. 6 (c) corresponds to these data, i.e., it represents the biplot corresponding to that of panel (a) but removing the contributions of the elements silicon, sulphur, calcium and potassium, thus only focusing on the elements responsible for the color of the postage stamps. Fig. 7, in turn, displays the respective dendrogram, using Ward's linkage. In all subsequent cluster analyses this same linkage method will be used, since it provides clear, distinctive, clusters. The colours attributed to the clusters correspond to those more frequently found in the samples gathered in each one. In the grey cluster, samples do not have a dominant colour.

In Fig. 7, upon inspection of the data, a good partitioning comprises 5

Table 2
Cluster composition of the dendrogram obtained with Ward's linkage for the average value for paper matrix of each sample. For labelling, please see [Table 1](#).

cluster number	Samples
(1)	#3, #7, #14, #15, #22
(2)	#4, #8, #13, #16, #17, #18, #19, #20, #21
(3)	#23, #26, #27, #28
(4)	#1, #24
(5)	#2, #5, #6, #9, #10, #11, #12, #25

clusters. Cluster (1) (in blue) is clearly separated from the other four and contains all the blue samples and two brown ones. Cluster (2) is, in turn, more heterogeneous. It now comprises lilac, rose, lilac rose, green and black samples. Cluster (3) is composed of three green, one rose and one brown sample. Moving further up along in the dendrogram, one can observe a cluster that is composed by the only yellow specimen (4). Finally, cluster (5) gathers greyish blue, ultramarine, orange, olive green, olive green yellowish, brown and lilac samples. Fig. 8 shows the average composition of the five clusters in the form of a circular bar plot.

This shows that cluster (1) is governed by the high content in iron, with some samples also containing lead and chlorine. The fact that the cluster involves blue and brown samples, the latter frequently resulting from a mixture with a blue pigment, suggests the existence of a common pigment in all samples, likely Prussian blue. This will be further confirmed by IR analysis (see below). Cluster (2) is composed by samples containing low amounts of the elements under inspection. For cluster (3), all samples display chlorine and a moderate amount of iron in their composition. Chromium and lead are present in the green samples, probably possessing chrome yellow (PbCrO_4) and Prussian blue pigments. The next cluster (4) is constituted by a single sample that is characterized by a high amount of zinc, which is consistent with the presence of the zinc yellow pigment ($\text{K}_2\text{O} \cdot 4\text{ZnCrO}_4 \cdot 3\text{H}_2\text{O}$). Finally, cluster (5) comprises samples with a high content of lead, except for one in which this content is moderate. Chlorine is also found in most of the samples. The presence of chlorine can be explained by the printing process that involves etching. Until the mid-1980s, the usual process of chemical etching made use of a ferric chloride solution, which corresponds to the source of chlorine [35].

Very interesting is to see that forgeries and postage stamps from the former Portuguese colonies are clustered according to the respective colour, and do not seem to behave as identifiable outliers.

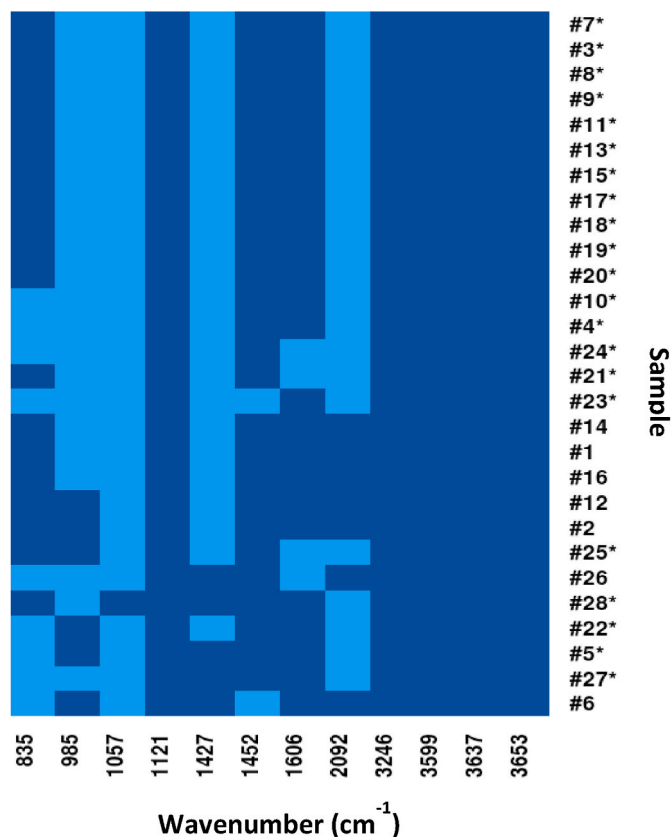


Fig. 9. Coincidence map with Prussian blue bands. Light blue indicates the presence of the band in the sample. Asterisk point to samples in which Prussian blue is likely to be present. For labelling, please see Table 1.

The clusters previously described (Fig. 7) can also be discerned in the biplot of Fig. 6 (c). The most prominent characteristics are that the cluster containing blue and brown samples (cluster 1) is found along the line of iron content, while cluster (5) accompanies the amount of the lead element present. The single yellow sample (lower right corner) of cluster (4) is responsible for the high zinc and chlorine loadings. The arrows in Fig. 6 (c) indicate these trends in iron, lead and zinc and chlorine.

In what concerns the paper matrix, a dendrogram based on the respective composition was also built to identify possible clusters. These are summarized in Table 2.

In this analysis of the paper matrix, it is seen that the colours of the samples do not contribute to the overall structure. This indicates that contamination from the dye/pigment is absent in most cases. Cluster (1) includes the samples with a high content of calcium and silicon. Cluster (2), in turn, gathers those with a higher content of calcium. Other elements, such as sulphur, are also detected in smaller amounts. The main components in cluster (3) are sulphur, silicon and barium, with the former clearly dominant. Cluster (4) comprises only two samples. Most elements are present in very low quantities and therefore not fulfilling the variability criterium. One of the samples contains lead (#6), but this element is also found in the pigment which points out to a probable contamination of the paper matrix. Several elements are present in cluster (5) with silicon and calcium dominating.

In terms of time periods, only clusters (2) and (3) gather samples for a narrow time period, i.e. essentially 1860's for the former and 1890's for the latter.

To interpret the ATR-FTIR obtained data, a database was created, where the wavenumber values, corresponding to the more important peaks, were grouped, i.e. aligned by columns of matching values, forming peak clusters. These clusters usually did not span more than 10 cm^{-1} . The results were confirmed using the K-means algorithm. This database was enlarged with literature information corresponding to reference materials such as cellulose, fillers and binders [27]. Approximately 100 products were taken into consideration (see list in Table S1 of supplementary material).

These data can be very easily transformed into binary information, in which the presence of a specific band is given by 1 and the absence by 0. The overall database shows a large number of common bands, found in both samples and reference materials. These cover a substantial part of the spectral range making difficult to have a fully automated recognition of the compounds present in the stamps.

The authors have created a script to guide in the identification of sample components. In this script, the characteristic bands of each reference (standard) material are used, and the matching bands, in the samples, consequently identified. The goal is to establish if the material is likely to be present in the samples. For that purpose, a table is built in which, for each characteristic band of the reference material, an indication is created, signalling absence or presence of that band in the sample spectra. This procedure is also used for the other standards, to check if the band is present. It is worth noting that, in affirmative cases, the band cannot be used to assign, unequivocally, a specific reference material.

In terms of dye/pigments, the colour and elemental content contribute to making the identification easier. This helps establishing a hypothesis on the presence of a specific compound in a specific set of samples. Subsequently, the presence of the vibrational transition (wavenumber value) corresponding to the compound considered is checked for the whole set of samples to validate the hypothesis.

However, the interpretation of these data is not, as expected, straightforward. Indeed, the presence of the cellulose matrix and the frequent superposition of peaks in different compounds obscure the results and calls for a systematic analysis.

To build the hypothesis, an initial set of candidates, extracted from the colour and elemental composition given by XRF, is considered. These include Prussian blue, chrome yellow, zinc yellow, litharge (PbO),

mar red (Fe_2O_3), red lead, lead sulphate and barium sulphate.

The above procedure is illustrated in Fig. 9. It presents a superposition map for Prussian blue. The hypothesis is that this pigment is present in the samples indicated with an asterisk. These are blue, brown and green samples, all of them containing iron.

In the case of Prussian blue, 13 bands were initially considered. Two of them are superimposed with cellulose bands corresponding to the stretching vibrations of the C–O groups in glucose chains (1057 and 1448 cm^{-1}) [13]. Those reported above 3200 cm^{-1} were not detected in any of the samples. Inspection of the remaining ones shows that the band with wavenumber at ca. 2092 cm^{-1} (C \equiv N stretching) [32] is present in all samples that contain iron and are of blue, brown and green colour. When one of these characteristic band is present, a straightforward analysis of the results, using a characteristic wavenumber value, can be applied. However, most potential inorganic pigments may not possess such distinctive bands, which does not allow structural identification through ATR-FTIR spectral analysis. This was the situation for all other remaining dye/pigments.

When proceeding to fillers, colour is not relevant in the characterization of the sample, but elemental composition is indispensable.

In the different samples, calcium was found to be present in two forms, calcite (CaCO_3) with two intense signals at 1412 (in-plane bending of CO_3^{2-}) and 870 cm^{-1} (asymmetric stretching of CO_3^{2-}) [36], and gypsum ($\text{CaSO}_4 \cdot 2\text{H}_2\text{O}$), mainly identified by the 3537 and 3400 cm^{-1} bands (OH stretching) [37]. XRF results indicate that out of the 28 samples under study, 22 possess calcium in its composition. Using the database created in this work, and the literature information on the more relevant bands, it was possible to identify 10 samples containing calcite and 4 containing gypsum. Eight of the samples, although containing calcium, did not exhibit the characteristic bands of gypsum or calcite.

Silicon is present in 21 samples, in the form of kaolinite ($\text{Al}_2\text{O}_3 \cdot 2\text{SiO}_2 \cdot 2\text{H}_2\text{O}$). A band at ca. 3694 cm^{-1} (Si–OH stretching) [15], characteristic of this compound, is visible in 18 of these samples. In the remaining ones, silicon is still present but in vestigial amounts.

In samples #1 and #19, the presence of kaolinite signal allows to distinguish between genuine specimen and forgeries. The latter lacks this component, which shows that a filler may provide evidence for identifying forgeries.

The barium present, in the form of barium sulphate, can be part of the printing ink or paper filler. The characteristic band, suggested in the literature for this compound, is found at ca. 634 cm^{-1} (out-of-plane bending vibration of the SO_4^{2-}) [38]. It cannot be assessed in these experiments, because the detector of the ATR-FTIR equipment only allows reliable determinations above 650 cm^{-1} . The spectrum of barium sulphate presents 4 other bands that can, in principle, be analysed. However, two of them coincide with bands from cellulose, matrix of the sample, and another is found in the Arabic gum spectrum. The band located at 1178 cm^{-1} (symmetrical vibration of the SO_4^{2-}) [38] allows

identification in most samples containing barium (5 in total), except for one (#19).

Most of the known binders are carbohydrates, proteins or waxes. There is a significant number of coinciding bands, which makes difficult to achieve definite identifications of different binders with ATR-FTIR. Protein glue and Arabic gum ($\text{C}_{15}\text{H}_{20}\text{NNaO}_4$) are common binders, in the time period considered [39]. As a consequence, its presence can also be evaluated. From literature data, both protein glue and Arabic gum can be identified by two bands, with a common at ca. 1650 cm^{-1} (amide I band associated with the C–N stretching and N–H bending vibrations of the peptide groups) [33,34]. As a result, the identification of each of these two binders will be based on the observation of both the common band and the discriminating one. For protein glue the discriminating band is at 1546 cm^{-1} corresponding to the amide II band. It is associated with the stretching of N–H and vibration of C–N [34]. For Arabic gum, the band at 1600 cm^{-1} is associated with COO^- anti-symmetric and symmetric stretching of carboxylate salts [40]. The latter does not coincide with those found in other binders. Most of the samples (20) contain protein glue, while in 3, Arabic gum could be detected. The distinction between these two compounds is not possible in two samples (#20 and #26). The remaining ones (5) do not show indication of possessing either protein glue or Arabic gum.

Table 3, summarizes the main findings for some of the postage stamp studied, joining the data and conclusions obtained from XRF, analysis and mapping, and ATR-FTIR. A full account of this information can be found in Table S2 of SI.

3.5. Additional remarks

Despite the UV–Vis technique did not provide enough information on the components that are present in each sample, it made possible, however, to distinguish genuine from fake samples. This technique allows for non-destructively identifying dyes/pigments, or at least to yield some level of discrimination. A draw-back is that, however, in most cases UV–Vis reflectance spectra do not show the degree of detail necessary for fingerprinting unknown materials [41]. The main problems are associated with the difficulty in dealing with spectral responses from mixtures of substances (e.g. mixtures of dyes/pigments). These responses can be less informative, especially in surfaces that are partially transparent, and colorants having similar absorption features are generally not possible to discriminate. In such cases, the additional use of other analytical techniques is mandatory.

XRF and ATR-FTIR worked as complementary techniques, one validating the results presented by the other and bringing further useful data. Indeed, interpretation of the ATR-FTIR data was achieved using a spectral database corresponding to ca. 100 reference materials, dye/pigments, fillers and binders. This allowed the automatic comparison between the spectra of the reference materials and that of the samples for the identification of the compounds that are present. It also permits

Table 3
Summary of main findings in samples presented in Fig. 1.

Sample	Color	Main content (XRF)	Mapping (XRF)	Components (XRF)	Main component peak (ATR-FTIR)	Components (ATR-FTIR)	Sample Constitution
2,1853-53 #3	Blue	Si, S, Cl, Ca, Fe, Pb	Fe delineates printing	Prussian blue ($\text{Fe}_4[\text{Fe}(\text{CN})_6]_3$)	2087 cm^{-1} 874 cm^{-1} 1548 and 1650 cm^{-1}	Prussian blue Calcite (CaCO_3) Protein glue	Prussian blue Calcite Protein glue
3,1853 #4	Green (blue+yellow+white)	Si, S, Cl, Ca, Cr, Fe, Pb	S, Cr, Fe (less visible), Pb delineate printing.	Prussian blue Chrome yellow (PbCrO_4) Lead sulphate (PbSO_4)	2098 cm^{-1} 3534 cm^{-1}	Prussian blue ($\text{Fe}_4[\text{Fe}(\text{CN})_6]_3$) Gypsum ($\text{CaSO}_4 \cdot 2\text{H}_2\text{O}$)	Prussian blue Chrome yellow Lead sulphate Gypsum
6,1855-56_un #7	Blue	Si, S, Ca, Fe, Pb	Fe delineates printing, S also (less visible)	Prussian blue ($\text{Fe}_4[\text{Fe}(\text{CN})_6]_3$) Lead sulphate (PbSO_4)	2088 cm^{-1} 3693 cm^{-1} 1548 and 1650 cm^{-1}	Prussian blue ($\text{Fe}_4[\text{Fe}(\text{CN})_6]_3$) Kaolinite ($\text{Al}_2\text{O}_3 \cdot 2\text{SiO}_2 \cdot 2\text{H}_2\text{O}$) Protein glue	Prussian blue Lead sulphate Kaolinite Protein glue

the observation of coinciding bands between reference materials making easier the selection of the most distinctive bands. The cellulose matrix makes the analysis of the results more difficult. It generates a series of bands overlapping with some of those from the remaining components. These were identified, in each case, so that other more distinctive peaks could be used to establish the reference material present in the sample. ATR-FTIR is, thus, particularly useful for identifying components that display bands at discriminating wavenumbers. Of all the dye/pigments present in the stamps of the current work, only Prussian blue could be identified due to the $C \equiv N$ stretching vibrational mode. This was possible even in cases where the iron content was very low and not fulfilling the variability criterion that was imposed. In contrast, four different types of fillers or coating pigments were detected (calcite, gypsum, kaolinite and barium sulphate). It was also possible to establish, in most samples, which binder was used (protein glue or Arabic gum).

XRF mapping provided unique information on the content of the paper and printed regions. In one of the samples it was also possible to establish the overall composition of the cancellation. This technique provides additional information on the function of certain components: if found on paper it can be mostly regarded as a filler, if found on the printed region, it can be classified as a dye/pigment.

The subsequent chemometric analysis allowed to determine the elements that, present in the paper, mask the composition of the pigments. Once these elements are removed, a clearer picture emerges, especially in the HCA results. These show clusters with distinctive compositions, coherent with the dye/pigments found in each one. In the paper matrix, it was clear that the respective content on calcium, silicon and sulphur and was responsible for the cluster structure.

In this work, a timeline establishing a correlation between the different components detected and those used at the time cannot yet be clearly established, essentially because there is a reduced number of pigments and dyes for dyeing the studied postage stamps. However, some findings can be here highlighted. Among the different blue dyes/pigments available in the time period considered in this work, only Prussian blue could be found [42].

Several yellow pigments could also have been found in the years considered, since they were used, at the time, for different painting purposes. However, the investigated Portuguese postage stamps show that only yellow ochre, litharge, chrome and zinc yellow could be detected in our samples [43,44].

In this work, the pigments found responsible for the red colour were mars red and red lead [45,46].

Additionally, we could detect the presence of two white pigments, lead and barium sulphate [47], and, at least, one black organic pigment.

In which regards fillers and coating pigments calcite, kaolinite and gypsum were found in the investigated postage stamps.

Finally, in what concerns the binders found in our samples, protein glue and Arabic gum, it is probable that Arabic gum appeared, in Portuguese postage stamps, only in 1880-81. Nevertheless, protein glue continued also to be used throughout the period considered.

4. Conclusion

A selected group of early Portuguese postage stamps was investigated using non-destructive analytical techniques (XRF, ATR-FTIR and UV-Vis), combined with multivariate tools (HCA, PCA) and including computer-aided data treatment for band recognition aiming to identify pigments, fillers, binders, and other materials used. The study shows that the colouring material is, in all studied postage stamps, almost totally of inorganic origin, which makes XRF the suitable technique to investigate the pigment composition of these stamps. Only five samples with possible organic dyes were identified. Combination of multiple analytical techniques with chemometrics provided extensive information on different aspects of the composition of the studied postage stamps. In all samples containing a blue pigment, Prussian blue was detected. It was observed that, in several cases, the final colour was

obtained by mixing different dye/pigments (up to three). This happened for brown, green and lilac samples. For example, sample #10 obtained the respective lilac colour from the mixture of blue, red and white pigments, respectively Prussian blue, red lead and lead sulphate.

Author's contributions

Simone Ferreira conducted all the experimental work (ATR-FTIR, XRF, UV-Vis) and analysis of the data, including chemometric analysis and the initial draft of the article.

Martina Franchi, performed part of the ATR-FTIR and XRF spectra of the studied postage stamps.

Alberto Canelas Pais, was responsible for the PCA and HCA programs and critical review of the data and final manuscript.

J. Sérgio Seixas de Melo, was responsible for the overall idea, structure and writing of the article, funding and supervision.

Declaration of competing interest

The authors declare that they have no known competing financial interests or personal relationships that could have appeared to influence the work reported in this paper.

Acknowledgments

The Coimbra Chemistry Centre (CQC) is supported by the Fundação para a Ciência e a Tecnologia (FCT, Portugal) through Projects UIDB/00313/2020 and UIDP/00313/2020. SF thanks FCT for PhD grant (UI/BD/150815/2021).

Appendix A. Supplementary data

Supplementary data to this article can be found online at <https://doi.org/10.1016/j.dyepig.2022.110519>.

References

- [1] Gómez-Jeria JS, Clavijo E. A preliminary infrared study of the cellulose of some world stamps. *J Chem Res* 2017;2:191-7.
- [2] Schwab NV, Da-Col JA, Meyer P, Bueno MIMS, Eberlin MN. Energy dispersive X-ray fluorescence profile of some Brazilian postage stamps. *J Braz Chem Soc* 2016; 27:1305-10.
- [3] Wood RE. Teaching francophonie with postage stamps. *Can Mod Lang Rev* 1979;36 (1):105-24.
- [4] Brunet F. Ben Franklin, America's postage stamp star — on the wane? *Transatlantica* 2009;2:1-10.
- [5] Chaplin TD, Jurado-López A, Clark RJH, Beech DR. Identification by Raman microscopy of pigments on early postage stamps: distinction between original 1847 and 1858-1862, forged and reproduction postage stamps of Mauritius. *J Raman Spectrosc* 2004;35(7):600-4.
- [6] Ferreira LE. A certain look at philately. 2006.
- [7] Hoisington WA. Politics and postage stamps: the postal issues of the French state and empire 1940-1944. *Fr Hist Stud* 1972;7(3):349-67.
- [8] Mota JM, Gonçalves R. Selos clássicos de Portugal : coleção de Albertino de Figueiredo. Madrid: Fundacion Albertino de Figueiredo para la Filatelia; 2005.
- [9] Pinto C, Seixas de Melo JS. The molecules of color in Portuguese postage stamps (1857-1909). *Pure Appl Chem* 2017;90(3):435-45. <https://doi.org/10.1515/pac-2017-0701>.
- [10] Conceição Oliveira Md, Dias A, Douglas P, Seixas de Melo JS. Perkin's and caro's mauveine in queen Victoria's lilac postage stamps: a chemical analysis. *Chem Eur J* 2014;20(7):1808-12.
- [11] Sharkey JB. Chemistry of postage stamps: dyes, phosphors, adhesives. *J Chem Educ* 1987;64(3):195-200.
- [12] Lera TM, Giaccai Jennifer A, Little Nicole. A scientific analysis of the first issues of Chile 1853-1862, london printing. In: *Proceedings of the first international symposium on analytical methods in philately*; 2013. p. 19-33.
- [13] Culasso N, Tomasini E. Spectral characterization of Argentine postage stamps using complementary in situ and non-invasive techniques. *Stud Conserv* 2021:1-11.
- [14] Castro K, Benito Á, Martínez-Arkarazo I, Etxebarria N, Madariaga JM. Scientific examination of classic Spanish stamps with colour error, a non-invasive micro-Raman and micro-XRF approach: the King Alfonso XIII (1889-1901 "Pelón") 15 cents definitive issue. *J Cult Herit* 2008;9(2):189-95.
- [15] Imperio E, Giancane G, Valli L. Spectral database for postage stamps by means of FT-IR spectroscopy. *Anal Chem* 2013;85(15):7085-93.

- [16] Eleonora Imperio GG, Valli Ludovico. Spectral database for postage stamps by means of FT-IR spectroscopy. *Spectrosc Eur* 2014;26:9–13.
- [17] Zhou W-h, Gan Q, Ji J-x, Yao N, Wang J-g, Zhou Z, et al. Non-destructive identification of pigments printed on six Imperial China Engraved Coiling Dragon stamps. *J Raman Spectrosc* 2016;47(3):316–20.
- [18] Araki S, Kondo E, Shibata T, Yokota T, Suzuki M, Hirashita T, et al. Analysis of pigments in the printing inks of the first Japanese postage stamps, the hand-engraved issues. *Bull Chem Soc Jpn* 2016;89:595–602.
- [19] Brittain HG. Attenuated total reflection fourier Transform infrared (ATR FT-IR) spectroscopy as a forensic method to determine the composition of inks used to print the United States one-cent blue Benjamin Franklin postage stamps of the 19th century. *Appl Spectrosc* 2016;70(1):128–36.
- [20] Gómez-Jeria JS, Campos-Vallette MM, Carrasco-Flores EA, Gutiérrez VS. Raman and X-ray fluorescence to identify colors of the German hyperinflation stamps of the 1923 collection. *J Chil Chem Soc* 2019;64:4622–6.
- [21] Akyuz T, Akyuz S. Investigations on Empire series postage stamps of Ottomans (printed 1880–1890) by vibrational spectroscopic and energy dispersive X-ray fluorescence techniques. *Vib Spectrosc* 2017;89:37–43.
- [22] Vaishnav S. Nondestructive authenticity of postage stamp: new approach in questioned document examination. *Indian J Appl Res* 2017;7(5):49.
- [23] Groß U. Forensic philately: the science of stamp authentication. *Chem Texts* 2018;4(4):18.
- [24] Melendez-Perez JJ, Correa DN, Hernandez VV, de Moraes DR, de Oliveira RB, de Souza W, et al. Forensic application of X-ray fluorescence spectroscopy for the discrimination of authentic and counterfeit revenue stamps. *Appl Spectrosc* 2016;70(11):1910–5.
- [25] Chaplin TD, Clark RJH, Beech DR. Comparison of genuine (1851–1852 AD) and forged or reproduction Hawaiian Missionary stamps using Raman microscopy. *J Raman Spectrosc* 2002;33(6):424–8.
- [26] *Classiques du monde 1840-1940*. 2005. In: Yvert et Tellier; 2005.
- [27] Vahur S, Teearu A, Peets P, Joosu L, Leito I. ATR-FT-IR spectral collection of conservation materials in the extended region of 4000–80 cm⁻¹. *Anal Bioanal Chem* 2016;408(13):3373–9.
- [28] Cosentino A. FORS spectral database of historical pigments in different binders. *Econ Serv J* 2014;2:57–68.
- [29] Almeida JAS, Barbosa LMS, Pais AACC, Formosinho SJ. Improving hierarchical cluster analysis: a new method with outlier detection and automatic clustering. *Chemometr Intell Lab Syst* 2007;87(2):208–17.
- [30] Is standard multivariate analysis sufficient in clinical and epidemiological studies? *J Biomed Inf* 2013;46(1):75–86.
- [31] Price SWT, Van Loon A, Keune K, Parsons AD, Murray C, Beale AM, et al. Unravelling the spatial dependency of the complex solid-state chemistry of Pb in a paint micro-sample from Rembrandt's Homer using XRD-CT. *Chem Commun* 2019;55(13):1931–4.
- [32] Rizzo A. Progress in the application of ATR-FTIR microscopy to the study of multi-layered cross-sections from works of art. *Anal Bioanal Chem* 2008;392(1–2):47–55.
- [33] Fant C, Hedlund J, Höök F, Berglin M, Fridell E, Elwing H. Investigation of adsorption and cross-linking of a mussel adhesive protein using attenuated total internal reflection fourier Transform infrared spectroscopy (ATR-FTIR). *J Adhes* 2010;86:25–38.
- [34] Rafe A, Razavi S. Effect of thermal treatment on chemical structure of B-lactoglobulin and basil seed gum mixture at different states by ATR-FTIR spectroscopy. *Int J Food Prop* 2015;18:2652–64.
- [35] Hind AM. A history of engraving and etching. New York: Courier Corporation; 2011.
- [36] Al-Hosney HA, Grassian VH. Water, sulfur dioxide and nitric acid adsorption on calcium carbonate: a transmission and ATR-FTIR study. *Phys Chem Chem Phys* 2005;7(6):1266–76.
- [37] Gunavathi P, Janaki D, Balasubramaniam P, Alagesan A, Geethanjali S. Characterization and identification of elemental sulphur, iron pyrite, mineral gypsum, Phospho gypsum and marine gypsum by using ATR-FTIR. *J Pharm Innov* 2021;10(5):80–6.
- [38] Ramaswamy V, Vimalathithan RM, Ponnusamy V. Synthesis and characterization of BaSO₄ nano-particles using micro-emulsion technique. *Adv Appl Sci Res* 2010;1:197–204.
- [39] Rouchon V, Bernard S. Mapping iron gall ink penetration within paper fibres using scanning transmission X-ray microscopy. *J Anal At Spectrom* 2015;30(3):635–41.
- [40] Degano I, Ribechini E, Modugno F, Colombini MP. Analytical methods for the characterization of organic dyes in artworks and in historical textiles. *Appl Spectrosc Rev* 2009;44(5):363–410.
- [41] Picollo M, Aceto M, Vitorino T. UV-Vis spectroscopy. *Phys Sci Rev* 2019;4(4):20180008.
- [42] Berke H. The invention of blue and purple pigments in ancient times. *Chem Soc Rev* 2007;36(1):15–30.
- [43] Berrie BH. Rethinking the history of artists' pigments through chemical analysis. *Annu Rev Anal Chem* 2012;5(1):441–59.
- [44] Agresti G, Baraldi P, Pelosi C, Santamaria U. Yellow pigments based on lead, tin, and antimony: ancient recipes, synthesis, characterization, and hue choice in artworks. *Color Res Appl* 2016;41(3):226–31.
- [45] Frano KA, Mayhew HE, Svoboda SA, Wustholz KL. Combined SERS and Raman analysis for the identification of red pigments in cross-sections from historic oil paintings. *Analyst* 2014;139(24):6450–5.
- [46] Čiuladienė A, Luckutė A, Kiuberis J, Kareiva A. Investigation of the chemical composition of red pigments and binding media. *Chemija* 2018;29.
- [47] Braun J, Koleske JV. White pigments. *Paint and Coating Testing Manual*. 15th. Philadelphia: ASTM International; 2012. p. 185–203. <https://doi.org/10.1520/MNL17-2ND-EB.978-0-8031-7017-9,0803170173>.